

Search for Heavy Neutral and Charged Leptons in e^+e^- Annihilation at $\sqrt{s} = 183$ and 189 GeV

The L3 Collaboration

Abstract

A search for unstable neutral and charged heavy leptons as well as for stable charged heavy leptons is performed at center-of-mass energies $\sqrt{s} = 183$ and 189 GeV with the L3 detector at LEP. No evidence for their existence is found. We exclude neutral heavy leptons which couple to the electron, muon or tau family, of the Dirac type for masses below 92.4, 93.3 and 83.3 GeV, and of the Majorana type for masses below 81.8, 84.1 and 73.5 GeV, respectively. We exclude unstable charged heavy leptons for masses below 93.9 GeV for a wide range of the associated neutral heavy lepton mass. If the unstable charged heavy lepton decays to a light neutrino, we exclude masses below 92.4 GeV. The production of stable charged heavy leptons with mass less than 93.5 GeV is also excluded.

Submitted to *Phys. Lett. B*

Introduction

Electron-positron colliders are well suited for the search for new heavy leptons with masses up to the beam energy [1]. Heavy leptons, L^\pm or L^0 , are pair-produced [2] through the s -channel: $e^+e^- \rightarrow \gamma/Z \rightarrow L^+L^-, L^0\bar{L}^0$. They are assumed to couple to the photon and the Z in the same way as the known leptons. The total expected cross sections are in the range of 1 to 4 pb at masses well below the beam energy and fall as the mass of the lepton approaches the beam energy. Here we report on a direct search for unstable sequential neutral heavy leptons (neutral partner to the charged lepton), L^0 , of the Dirac or Majorana type, and charged heavy leptons, L^\pm , updating our previous search [3]. Other recent results on this subject obtained at LEP at $\sqrt{s} = 133$ to 183 GeV, can be found in reference [4]. The data used in this analysis were collected with the L3 detector at LEP at $\sqrt{s} = 183$ GeV with an integrated luminosity of 56 pb^{-1} , and at $\sqrt{s} = 189$ GeV with an integrated luminosity of 176 pb^{-1} . We have combined the results with our earlier data recorded at $\sqrt{s} = 133$ to 172 GeV. The L3 detector is described elsewhere [5].

The neutral heavy lepton is expected to decay to a light lepton $L^0 \rightarrow \ell^\pm W^{\mp*}$, ($\ell = e, \mu, \tau$). In this search we consider only the case where both neutral heavy leptons decay to the same lepton family (electron, muon, or tau). In this case, the decay amplitude contains a parameter U for the transition from the heavy lepton to the light lepton. The mean decay length, D , is given by [6] $D = \beta\gamma c\tau_L \propto \beta|U|^{-2}m_L^\alpha$, where m_L is the mass and τ_L is the lifetime of the heavy lepton and $\alpha \approx -6$. To ensure high detection and reconstruction efficiencies, the search is restricted to neutral leptons decaying within 1 cm of the interaction point. This limits the sensitivity to the transition parameter to $|U|^2 > \mathcal{O}(10^{-12})$.

Three different possibilities for the charged heavy lepton decay modes are considered:

- 1) The charged lepton decays via a lepton-number-nonconserving interaction to light neutrinos, $L^\pm \rightarrow \nu_\ell W^{\pm*}$.
- 2) The charged lepton decays through a lepton-number-conserving weak charged current interaction, $L^\pm \rightarrow L^0 W^{\pm*}$, with L^0 being stable.
- 3) The charged lepton is stable. This is the case if the associated neutral lepton is heavier than its charged partner and there is no or very small probability to decay into light neutrinos.

Event Simulation

The generation of heavy leptons and their decay is performed with the TIPTOP [7] Monte-Carlo program which takes into account initial state radiation and spin effects. For the search we consider the mass range of the heavy leptons between 50 and 94 GeV. For the simulation of background from Standard Model processes the following Monte-Carlo programs are used: PYTHIA 5.7 [8] ($e^+e^- \rightarrow q\bar{q}(\gamma)$, Ze^+e^- , ZZ), KORALZ [9] ($e^+e^- \rightarrow \tau^+\tau^-(\gamma)$), KORALW [10] ($e^+e^- \rightarrow W^+W^-$), PHOJET [11] ($e^+e^- \rightarrow e^+e^-q\bar{q}$), DIAG36 [12] ($e^+e^- \rightarrow e^+e^-\tau^+\tau^-$), and EXCALIBUR [13] ($e^+e^- \rightarrow f\bar{f}f\bar{f}$). The Monte-Carlo events are simulated in the L3 detector using the GEANT3 program [14], which takes into account the effects of energy loss, multiple scattering and showering in the materials.

Search for Unstable Neutral Heavy Leptons

The event topology used in the search for pair produced neutral heavy leptons is two isolated leptons (e , μ , or τ) of the same family plus the decay products of real or virtual W bosons, i.e. $e^+e^- \rightarrow L^0\bar{L}^0 \rightarrow \ell^+\ell^-W^{+*}W^{-*}$. Hadronic events with visible energy greater than 60 GeV and charged track multiplicity greater than 3 are used in this analysis. The search follows closely the procedure described previously [3].

For the case where both neutral heavy leptons decay to either electrons or muons, events must also satisfy the following criteria:

- The number of reconstructed jets plus isolated leptons is at least 3.
- The energy sum of the two isolated electrons or muons must be less than 70 GeV. This is a cut introduced to reject the Z-pair background. Figure 1a) shows an example of the isolation criteria.

After applying the selection, 6 events remain in the 189 GeV data for the electron decay mode while 7.2 ± 0.5 background events are expected. For the muon decay mode, 1 event remains in the 189 GeV data while 1.2 ± 0.2 background events are expected. For the 183 GeV data, 1 event satisfies the selection requirements for the electron decay mode and none for the muon decay mode while 1.8 ± 0.2 and 0.9 ± 0.1 background events are expected, respectively.

For the case where both neutral heavy leptons decay to tau leptons, each of the taus can independently decay to hadrons, muons, or electrons. When both tau leptons decay to either muons or electrons, the above selection is applied with the exception that we allow the isolated leptons to be either two electrons, two muons, or one muon and one electron. We also consider the final state in which at least one of the tau decays into one charged hadron. In this case, events satisfying the following criteria are selected:

- The number of reconstructed jets plus isolated leptons is at least 4.
- The polar angle (angle with the beam axis) θ of the missing momentum must be in the range $25^\circ < \theta < 155^\circ$, and the fraction of visible energy in the forward-backward region ($\theta < 20^\circ$ and $\theta > 160^\circ$) must be less than 40%.
- The angle between the most isolated track and the track nearest to it, must be greater than 50° or the angle between the second most isolated track and the track nearest to it, must be greater than 25° . The transverse momenta, p_t , of the two most isolated tracks must be greater than 1.2 GeV, and at least one track must have p_t greater than 2.5 GeV.
- The visible energy is required to be less than 175 GeV.
- The electron and muon energies must be less than 40 GeV.

After applying the above selection, 33 events remain in the 189 GeV data, while 32.3 ± 1.0 background events are expected. For the 183 GeV data, 5 events satisfy the selection requirements while 6.8 ± 0.3 background events are expected.

The selection efficiencies are determined by Monte-Carlo. For neutral heavy leptons in the vicinity of the mass limit from 80 to 94 GeV, it is 28.0% to 33.5% for the electron decay mode. For the muon decay mode the efficiency in the same mass range is 25.0% to 32.2%. For the tau decay mode, the selection efficiency ranges from 23.4% for 70 GeV to 17.3% for 85 GeV.

The systematic error, which is mainly due to the uncertainties in the energy calibration factors and the lepton identification efficiency and purity, is estimated to be 5% relative. To obtain exclusion limits in this and subsequent analyses, the selection efficiency has been reduced by one standard deviation in the total systematic error. Taking into account the luminosity, the selection efficiency and the production cross section we obtain a lower limit on the neutral heavy lepton mass using the procedure from reference [15]. Combining this result with our previous analysis [3] we exclude at 95% C.L. the production of unstable neutral heavy leptons of the Dirac type for masses below 92.4, 93.3 and 83.3 GeV and of the Majorana type below 81.8, 84.1 and 73.5 GeV, if the neutral heavy lepton couples to the electron, muon and tau family, respectively. These results are summarized in Table 1.

Search for Unstable Charged Heavy Leptons

Decay into a light neutrino, $L^\pm \rightarrow \nu_\ell W^{\pm*}$

For this search, two sets of cuts are used to search for the topology with one hadronic and one leptonic W-decay as well as two hadronic W-decays. For both selections we require that the visible energy be greater than 50 GeV, the multiplicity of charged tracks be greater than 3, and the fraction of the total visible energy in the forward-backward region be less than 25%.

For the mode $L^+L^- \rightarrow \nu_\ell\bar{\nu}_\ell W^{+*}W^{-*} \rightarrow \nu_\ell\bar{\nu}_\ell\ell\nu_\ell q\bar{q}'$, events satisfying the following criteria are selected:

- The event contains at least one isolated electron or muon with energy greater than 4 GeV and less than 50 GeV.
- The number of reconstructed jets plus isolated leptons is at least 3.
- The polar angle θ of the missing momentum must be in the range $25^\circ < \theta < 155^\circ$.
- The sum of the energies of the hadronic jets must be less than 80 GeV. Figure 1b) shows the distribution of the sum of the energies of hadronic jets, after all other cuts have been applied.

After applying the selection, 20 events remain in the 189 GeV data while 23.2 ± 0.8 background events are expected. To set mass limits, only the 189 GeV data are utilized since the lower energy data does not contribute significantly to the setting of the limit.

For the mode where both W bosons decay hadronically, events satisfying the following criteria are selected:

- The event does not contain any isolated electrons or muons and the energy of each non-isolated electron or muon must be less than 30 GeV.
- The number of hadronic jets is at least 4.

For charged heavy lepton masses greater than the W boson mass, the leptons each decay to a real W. The dominant remaining background after the previous cuts have been applied is W-pair production. However, for the signal events, due to the energy and momentum carried away by light neutrinos, the total visible energy is less than \sqrt{s} and the two W bosons are not back-to-back. To improve the determination of jet energies and angles (both for the signal and

the background) a kinematic fit is applied imposing the constraint that both jet-jet invariant masses are equal to the W mass. All possible jet-jet combinations are considered and the one which gives the smallest χ^2 of the fit is chosen. The following additional requirements are then imposed for the case where the charged lepton mass is greater than 80 GeV:

- The visible energy must be less than $\sqrt{s} - 10$ GeV. Figure 1c) shows the distribution of visible energy, after all previous cuts have been applied.
- The angle between the two W candidates is less than 160° .
- The total transverse momentum of jets must be greater than 10 GeV. Figure 1d) shows the distribution of this quantity, after all other cuts have been applied.

After applying the selection, 51 events remain in 189 GeV data while 53.3 ± 1.5 background events are expected. To set mass limits only the 189 GeV data are utilized since the lower energy data does not contribute significantly to the setting of the limit.

The kinematic distributions of the candidates from both topologies are consistent with those expected from background. The selection efficiency for 90 GeV charged heavy leptons is 17.9%. The systematic error, which is mainly due to the uncertainties in the energy calibration factors and the lepton identification efficiency and purity, is estimated to be 5% relative. Taking into account the luminosity, the selection efficiency and the production cross section we obtain a lower limit on the charged heavy lepton mass using the procedure from reference [15]. We exclude the production of unstable charged heavy leptons at 95% C.L. for masses below 92.4 GeV. The results of this search are summarized in Table 1.

Decay into stable neutral heavy lepton, $L^\pm \rightarrow L^0 W^{\pm*}$

In this case the charged lepton decays into its associated neutral lepton L^0 . From LEP results at the Z resonance [16], the mass of the stable L^0 must be greater than 40 GeV, thus the signal events are characterized by a large missing energy and a large transverse momentum imbalance. In the limit of a vanishing mass difference between charged lepton and associated neutral lepton ($\Delta m = m_{L^\pm} - m_{L^0}$), the sensitivity to the signal is limited by the trigger efficiency and the large two-photon background. Hence, the search is restricted to $10 \text{ GeV} \leq \Delta m \leq 45 \text{ GeV}$. The case of a light neutral lepton ($\Delta m = m_{L^\pm}$) has been considered in the previous section. The main background is the two-photon process for small mass difference ($\Delta m \leq 20 \text{ GeV}$) and the $q\bar{q}(\gamma)$ and WW processes for high mass difference ($\Delta m \geq 20 \text{ GeV}$).

The above signature of a charged heavy lepton is very similar to that of a chargino, when the chargino decays into a stable neutralino and a W boson. Therefore, we use a selection developed for the chargino search [17], which is mainly based on the signatures of missing energy, transverse momentum imbalance, missing mass, acoplanarity and isolated leptons.

After applying the selection, 9 events remain in the 189 GeV data while 9.9 ± 1.5 events are expected from background. Only the 189 GeV data are utilized since the lower energy data does not contribute significantly to the setting of the limit.

The selection efficiency varies from $\sim 5\%$ for $\Delta m = 10 \text{ GeV}$ to 40% for $\Delta m = 45 \text{ GeV}$. The typical systematic error, which is mainly due to the Monte-Carlo statistics and to uncertainties in energy calibration factors and jet angular resolution, is estimated to be 5% relative. Taking into account the luminosity, selection efficiency and the production cross section we obtain a lower limit on the charged heavy lepton mass. Figure 2 shows the 95% C.L. exclusion contour in the $m_{L^\pm} - m_{L^0}$ plane. The exclusion region extends to $m_{L^\pm} = 93.9 \text{ GeV}$. The result of this search is summarized in Table 1.

Search for Stable Charged Heavy Leptons

This search is designed for stable charged particles with masses from 45 GeV up to the beam energy, E_B . The search uses all the data from $\sqrt{s} = 133$ GeV to 189 GeV, and follows closely the procedure described in reference [18] for the stable slepton-pair search. The main difference between the two analyses is that the efficiency is greater for sleptons which have a different angular distribution than fermions. The search is performed with selection requirements optimized for three different mass regions: high ($m_L/E_B > 0.8$), intermediate ($0.7 < m_L/E_B < 0.8$) and low ($0.5 < m_L/E_B < 0.7$).

Events are selected which have two charged tracks with momentum greater than 5 GeV and polar angle $|\cos\theta| < 0.82$. The acollinearity angle between the two tracks is required to be less than 15° . The polar angle requirement selects events where the trigger and track reconstruction efficiency is high and the dE/dx resolution in the tracking chamber is good. The momentum and acollinearity angle cuts reduce the background from two photon produced lepton pairs as well as from dilepton annihilation events with a high energy photon in the final state.

In the region $m_L/E_B > 0.8$, the stable leptons are highly ionizing and only the tracking chamber information is utilized. The dE/dx measurement is calibrated with Bhabha scattering events, and the mean value of the resulting dE/dx distribution is normalized to one. Its resolution is 0.08. Events are selected for which the ionization energy loss for each track is between 1.25 and 8, and the product of the track ionization losses is larger than 2.

Figure 3 shows the dE/dx measurements of the first and second tracks for data events at 189 GeV passing all cuts except those on track ionization, as well as the simulated signal from pair-production of 93 GeV stable charged leptons. One candidate event satisfies the selection requirements in the 189 GeV data and none in the lower energy data samples. The candidate event in the data corresponds to pair production of stable charged particles of mass $80_{-2.5}^{+1.5}$ GeV. The background is estimated to be less than 0.5 events at the 90% C.L. for the entire data sample. We have conservatively assumed that there are no background events when producing exclusion limits in this region.

The efficiency for selection of heavy stable charged leptons ranges from 58% to 70% over the range $0.8 < m_L/E_B < 0.99$. For $m_L/E_B > 0.99$, the charged particles are very highly ionizing and saturation effects become significant and may lead to track reconstruction inefficiencies. The ionization has been studied using low energy protons in our hadronic events up to 8 units in dE/dx which corresponds to $m_L/E_B = 0.99$.

In the region $0.7 < m_L/E_B < 0.8$, we combine the information from the dE/dx and the muon chambers to search for stable heavy leptons. Events are required to satisfy the following criteria: the matched energy deposit in the electromagnetic calorimeter is less than 2 GeV for each track; the ionization energy loss for each track is greater than 1.05, their product is larger than 1.25, and there is at least one track in the muon chamber with $p/E_B > 0.4$.

One candidate event is observed in the 189 GeV data sample and none in the lower energy data samples. From the dE/dx information, the candidate event is consistent with pair production of mass 64 ± 3 GeV stable charged particles. The total background in the entire data sample is estimated to be 1.1 ± 0.2 events of which 0.6 events are expected in the 189 GeV data. This background is taken into account in producing exclusion limits. The selection efficiency ranges from 34% at $m_L/E_B = 0.7$ to 58% at $m_L/E_B = 0.8$.

In the region $0.5 < m_L/E_B < 0.7$, the dE/dx ionization is indistinguishable from that of lighter particles. Consequently, only the muon chamber momentum and calorimeter information are used. Assuming the energy of the particles is E_B , the momentum of the track can be used

Table 1: Mass limits from the various heavy lepton search channels.

Channel	95% CL Mass Limit GeV	
	Dirac	Majorana
L^0		
$L^0 \rightarrow eW$	92.4	81.8
$L^0 \rightarrow \mu W$	93.3	84.1
$L^0 \rightarrow \tau W$	83.3	73.5
$L^\pm \rightarrow \nu_\ell W^{\pm*}$	92.4	
$L^\pm \rightarrow L^0 W^{\pm*}$	93.9	
Stable L^\pm	93.5	

to reconstruct the mass of the heavy particle: $m_L = \sqrt{E_B^2 - p^2}$. Events are selected which satisfy the following criteria: two tracks are found in the muon spectrometer in the polar angle range $|\cos\theta| < 0.76$, each with $0.55 < p/E_B < 1.0$; the acollinearity angle between the tracks is less than 10° ; the matched energy deposit in the electromagnetic calorimeter is less than 2 GeV and that in the hadronic calorimeter less than 15 GeV for each track; the sum of the unmatched electromagnetic calorimeter energy deposits is less than 1 GeV; the reconstructed mass using the muon chamber momentum for each particle exceeds 45 GeV.

Three events pass the selection requirements in the 189 GeV data and none in the lower energy data samples. The background is estimated to be 3.3 ± 0.1 events in the entire data sample of which 2.6 events are expected in the 189 GeV data, mostly from dimuon events. The background is taken into account in determining exclusion limits from the data. The selection efficiency ranges from 9% at $m_L/E_B = 0.5$ to 34% at $m_L/E_B = 0.7$.

The upper limit on the number of signal events over the entire mass range 45 GeV to 93.5 GeV has been converted to an upper limit on the production cross section using the luminosity of the data and the selection efficiency. The systematic error, estimated to be 5% relative, is mainly due to the Monte-Carlo statistics.

Figure 4 shows the upper limit of the cross section obtained from the combined 133 GeV to 189 GeV data. The candidate events are accounted for by using a range of $\pm 2\sigma$ in the uncertainty in the mass centered about the mass corresponding to the observed events. The 95% CL. upper limit on the production cross section for pair production of stable heavy leptons is 0.08-0.02 pb for the mass range 50 to 93.5 GeV and less than 0.18 pb for the mass range 45 to 50 GeV. We do not quote an upper limit for masses greater than 93.5 GeV.

Figure 4 also shows the calculated cross section [7] for heavy charged leptons as a function of mass at $\sqrt{s} = 189$ GeV. From the comparison of the two curves, we exclude production of stable heavy charged leptons with mass less than 93.5 GeV at 95% C.L. and this result is included in Table 1.

Acknowledgements

We wish to express our gratitude to the CERN accelerator divisions for the excellent performance of the LEP machine. We acknowledge with appreciation the effort of the engineers, technicians and support staff who have participated in the construction and maintenance of this experiment.

Author List

The L3 Collaboration:

M.Acciarri²⁵ P.Achard¹⁸ O.Adriani¹⁵ M.Aguilar-Benitez²⁴ J.Alcaraz²⁴ G.Alemanni²¹ J.Allaby¹⁶ A.Aloisio²⁷
M.G.Alvigi²⁷ G.Ambrosi¹⁸ H.Anderhub⁴⁶ V.P.Andreev^{6,35} T.Angelescu² F.Anselmo⁹ A.Arefiev²⁶ T.Azmoon³
T.Aziz¹⁰ P.Bagnaia³⁴ L.Baksay⁴¹ A.Balandras⁴ R.C.Ball³ S.Banerjee¹⁰ Sw.Banerjee¹⁰ A.Barczyk^{46,44}
R.Barillère¹⁶ L.Barone³⁴ P.Bartalini²¹ M.Basile⁹ R.Battiston³¹ A.Bay²¹ F.Becattini¹⁵ U.Becker¹⁴ F.Behner⁴⁶
J.Berdugo²⁴ P.Berges¹⁴ B.Bertucci³¹ B.L.Betev⁴⁶ S.Bhattacharya¹⁰ M.Biasini³¹ A.Biland⁴⁶ J.J.Blaising⁴
S.C.Blyth³² G.J.Bobbink² A.Böhm¹ L.Boldizsar¹³ B.Borgia³⁴ D.Bourilkov⁴⁶ M.Bourquin¹⁸ S.Braccini¹⁸
J.G.Branson³⁷ V.Brigljevic⁴⁶ F.Brochu⁴ A.Buffini¹⁵ A.Buijs⁴² J.D.Burger¹⁴ W.J.Burger³¹ J.Busenitz⁴¹
A.Button³ X.D.Cai¹⁴ M.Campanelli⁴⁶ M.Capell¹⁴ G.Cara Romeo⁹ G.Carlino²⁷ A.M.Cartacci¹⁵ J.Casaus²⁴
G.Castellini¹⁵ F.Cavallari³⁴ N.Cavallo²⁷ C.Cecchi¹⁸ M.Cerrada²⁴ F.Cesaroni²² M.Chamizo¹⁸ Y.H.Chang⁴⁸
U.K.Chaturvedi¹⁷ M.Chemarin²³ A.Chen⁴⁸ G.Chen⁷ G.M.Chen⁷ H.F.Chen¹⁹ H.S.Chen⁷ X.Chereau⁴ G.Chiefari²⁷
L.Cifarelli³⁶ F.Cindolo³ C.Civinini¹⁵ I.Clare¹⁴ R.Clare¹⁴ G.Coignet⁴ A.P.Colijn² N.Colino²⁴ S.Costantini⁸
F.Cotorobai¹² B.Cozzoni⁹ B.de la Cruz²⁴ A.Csilling¹³ S.Cucciarelli³¹ T.S.Dai⁴ J.A.van Dalen²⁹
R.D'Alessandro¹⁵ R.de Asmundis²⁷ P.Deglon¹⁸ A.Degré⁴ K.Deiters⁴⁴ D.della Volpe²⁷ P.Denes³³
F.DeNotaristefani³⁴ A.De Salvo⁴⁶ M.Diemoz³⁴ D.van Dierendonck² F.Di Lodovico⁴⁶ C.Dionisi³⁴ M.Dittmar⁴⁶
A.Dominguez³⁷ A.Doria²⁷ M.T.Dova^{17,‡} D.Duchesneau⁴ D.Dufourmand⁴ P.Duinker² I.Duran³⁸ H.El Mamouni²³
A.Engler³² F.J.Eppling¹⁴ F.C.Erné² P.Extermann¹⁸ M.Fabre⁴⁴ R.Faccini³⁴ M.A.Falagan²⁴ S.Falciano^{34,16}
A.Favara¹⁶ J.Fay²³ O.Fedin³⁵ M.Felcini⁴⁶ T.Ferguson³² F.Ferroni³⁴ H.Fesefeldt¹ E.Fiandrini³¹ J.H.Field¹⁸
F.Filthaut¹⁶ P.H.Fisher¹⁴ I.Fisk³⁷ G.Forconi¹⁴ L.Fredj¹⁸ K.Freudenreich⁴⁶ C.Furetta²⁵ Yu.Galaktionov^{26,14}
S.N.Ganguli¹⁰ P.Garcia-Abia⁵ M.Gataullin³⁰ S.S.Gau¹¹ S.Gentile^{34,16} N.Gheordanescu¹² S.Giagu³⁴ Z.F.Gong¹⁹
G.Grenier²³ O.Grimm⁴⁶ M.W.Gruenewald⁸ R.van Gulik² V.K.Gupta³³ A.Gurtu¹⁰ L.J.Gutay⁴³ D.Haas⁵
A.Hasan²⁸ D.Hatzifotiadou⁹ T.Hebbeker⁸ A.Hervé¹⁶ P.Hidas¹³ J.Hirschfelder³² H.Hofer⁴⁶ G.Holzner⁴⁶
H.Hoorani³² S.R.Hou⁴⁸ I.Iashvili⁴⁵ B.N.Jin⁷ L.W.Jones³ P.de Jong² I.Josa-Mutuberria²⁴ R.A.Khan¹⁷
D.Kamrad⁴⁵ M.Kaur^{17,◇} M.N.Kienzle-Focacci¹⁸ D.Kim³⁴ D.H.Kim⁴⁰ J.K.Kim⁴⁰ S.C.Kim⁴⁰ J.Kirkby¹⁶ D.Kiss¹³
W.Kittel²⁹ A.Klimentov^{14,26} A.C.König²⁹ A.Kopp⁴⁵ I.Korolko²⁶ V.Koutsenko^{14,26} M.Kräber⁴⁶ R.W.Kraemer³²
W.Krenz¹ A.Kunin^{14,26} P.Lacetre^{45,‡,‡} P.Ladron de Guevara²⁴ I.Laktinel²³ G.Landi¹⁵ K.Lassila-Perini⁴⁶
P.Laurikainen²⁰ A.Lavorato³⁶ M.Lebeau¹⁶ A.Lebedev¹⁴ P.Lebrun²³ P.Lecomte⁴⁶ P.Lecoq¹⁶ P.Le Coultre⁴⁶
H.J.Lee⁸ J.M.Le Goff¹⁶ R.Leiste⁴⁵ E.Leonardi³⁴ P.Levtchenko³⁵ C.Li¹⁹ C.H.Lin⁴⁸ W.T.Lin⁴⁸ F.L.Linde²
L.Lista²⁷ Z.A.Liu⁷ W.Lohmann⁴⁵ E.Longo³⁴ Y.S.Lu⁷ K.Lübelsmeyer¹ C.Luci^{16,34} D.Luckey¹⁴ L.Lugnier²³
P.Luminari³⁴ W.Lustermann⁴⁶ W.G.Ma¹⁹ M.Maity¹⁰ L.Malgeri¹⁶ A.Malinin^{26,16} C.Maña²⁴ D.Mangeol²⁹
L.Marchesini⁴⁶ G.Marian^{41,¶} J.P.Martin²³ F.Marzano³⁴ G.G.G.Massaro² K.Mazumdar¹⁰ R.R.McNeil⁶ S.Mele¹⁶
L.Merola²⁷ M.Meschini¹⁵ W.J.Metzger²⁹ M.von der Mey¹ D.Migani⁹ A.Mihul¹² H.Milcent¹⁶ G.Mirabella³⁴
J.Mnich¹⁶ G.B.Mohanty¹⁰ P.Molnar⁸ B.Monteoloni¹⁵ T.Moulik¹⁰ G.S.Muanza²³ F.Muheim¹⁸ A.J.M.Muijs²
M.Napolitano²⁷ F.Nessi-Tedaldi⁴⁶ H.Newman³⁰ T.Niessen¹ A.Nisati³⁴ H.Nowak⁴⁵ Y.D.Oh⁴⁰ G.Organtini³⁴
R.Ostonen²⁰ C.Palomares²⁴ D.Pandoulas¹ S.Paoletti^{34,16} P.Paolucci²⁷ H.K.Park³² I.H.Park⁴⁰ G.Pascale³⁴
G.Passaleva¹⁶ S.Patricelli²⁷ T.Paul¹¹ M.Pauluzzi³¹ C.Paus¹⁶ F.Pauss⁴⁶ D.Peach¹⁶ M.Pedace³⁴ Y.J.Pei¹
S.Pensotti²⁵ D.Perret-Gallix⁴ B.Petersen²⁹ D.Piccolo²⁷ M.Pieri¹⁵ P.A.Piroué³³ E.Pistoiesi²⁵ V.Plyaskin²⁶
M.Pohl⁴⁶ V.Pojidaev^{26,15} H.Postema¹⁴ J.Pothier¹⁶ N.Produit¹⁸ D.O.Prokofiev⁴³ D.Prokofiev³⁵ J.Quartieri³⁶
G.Rahal-Callot^{46,16} M.A.Rahaman¹⁰ N.Raja¹⁰ R.Ramelli⁴⁶ P.G.Rancoita²⁵ G.Raven³⁷ P.Razis²⁸ D.Ren⁴⁶
M.Rescigno³⁴ S.Reucroft¹¹ T.van Rhee⁴² S.Riemann⁴⁵ K.Riles³ A.Robohm⁴⁶ J.Rodin⁴¹ B.P.Roe³ L.Romero²⁴
A.Rosca⁸ S.Rosier-Lees⁴ J.A.Rubio¹⁶ D.Ruschmeier⁸ H.Ryckaczewski⁴⁶ S.Sarkar³⁴ J.Salicio¹⁶ E.Sanchez¹⁶
M.P.Sanders²⁹ M.E.Sarakinos²⁰ C.Schäfer¹ V.Schegelsky³⁵ S.Schmidt-Kaerst¹ D.Schmitz¹ H.Schopper⁴⁷
D.J.Schotanus²⁹ J.Schwenke¹ G.Schwering¹ C.Sciacca²⁷ D.Sciarrino¹⁸ A.Seganti⁹ L.Servoli³¹ S.Shevchenko³⁰
N.Shivarov³⁹ V.Shoutko²⁶ E.Shumilov²⁶ A.Shvorob³⁰ T.Siedenburg¹ D.Son⁴⁰ B.Smith³² P.Spillantini¹⁵
M.Steuer¹⁴ D.P.Stickland³³ A.Stone⁶ H.Stone³³ B.Stoyanov³⁹ A.Straessner¹ K.Sudhakar¹⁰ G.Sultanov¹⁷
L.Z.Sun¹⁹ H.Suter⁴⁶ J.D.Swain¹⁷ Z.Szillasi^{41,¶} X.W.Tang⁷ L.Tauscher⁵ L.Taylor¹¹ C.Timmermans²⁹
Samuel C.C.Ting¹⁴ S.M.Ting¹⁴ S.C.Tonwar¹⁰ J.Tóth¹³ C.Tully³³ K.L.Tung⁷ Y.Uchida¹⁴ J.Ulbricht⁴⁶ E.Valente³⁴
G.Vesztegombi¹³ I.Vetlitsky²⁶ D.Vicinanza³⁶ G.Viertel⁴⁶ S.Villa¹¹ M.Vivargent⁴ S.Vlachos⁵ I.Vodopianov³⁵
H.Vogel³² H.Vogt⁴⁵ I.Vorobiev²⁶ A.A.Vorobyov³⁵ A.Vorvolakos²⁸ M.Wadhwa⁵ W.Wallraff¹ M.Wang¹⁴
X.L.Wang¹⁹ Z.M.Wang¹⁹ A.Weber¹ M.Weber¹ P.Wienemann¹ H.Wilkens²⁹ S.X.Wu¹⁴ S.Wynhoff¹ L.Xia³⁰
Z.Z.Xu¹⁹ B.Z.Yang¹⁹ C.G.Yang⁷ H.J.Yang⁷ M.Yang⁷ J.B.Ye¹⁹ S.C.Yeh⁴⁹ J.M.You³² An.Zalite³⁵ Yu.Zalite³⁵
Z.P.Zhang¹⁹ G.Y.Zhu⁷ R.Y.Zhu³⁰ A.Zichichi^{9,16,17} F.Ziegler⁴⁵ G.Zilizi^{41,¶} M.Zöller¹

- 1 I. Physikalisches Institut, RWTH, D-52056 Aachen, FRG[§]
III. Physikalisches Institut, RWTH, D-52056 Aachen, FRG[§]
 - 2 National Institute for High Energy Physics, NIKHEF, and University of Amsterdam, NL-1009 DB Amsterdam, The Netherlands
 - 3 University of Michigan, Ann Arbor, MI 48109, USA
 - 4 Laboratoire d'Annecy-le-Vieux de Physique des Particules, LAPP, IN2P3-CNRS, BP 110, F-74941 Annecy-le-Vieux CEDEX, France
 - 5 Institute of Physics, University of Basel, CH-4056 Basel, Switzerland
 - 6 Louisiana State University, Baton Rouge, LA 70803, USA
 - 7 Institute of High Energy Physics, IHEP, 100039 Beijing, China[△]
 - 8 Humboldt University, D-10099 Berlin, FRG[§]
 - 9 University of Bologna and INFN-Sezione di Bologna, I-40126 Bologna, Italy
 - 10 Tata Institute of Fundamental Research, Bombay 400 005, India
 - 11 Northeastern University, Boston, MA 02115, USA
 - 12 Institute of Atomic Physics and University of Bucharest, R-76900 Bucharest, Romania
 - 13 Central Research Institute for Physics of the Hungarian Academy of Sciences, H-1525 Budapest 114, Hungary[‡]
 - 14 Massachusetts Institute of Technology, Cambridge, MA 02139, USA
 - 15 INFN Sezione di Firenze and University of Florence, I-50125 Florence, Italy
 - 16 European Laboratory for Particle Physics, CERN, CH-1211 Geneva 23, Switzerland
 - 17 World Laboratory, FBLJA Project, CH-1211 Geneva 23, Switzerland
 - 18 University of Geneva, CH-1211 Geneva 4, Switzerland
 - 19 Chinese University of Science and Technology, USTC, Hefei, Anhui 230 029, China[△]
 - 20 SEFT, Research Institute for High Energy Physics, P.O. Box 9, SF-00014 Helsinki, Finland
 - 21 University of Lausanne, CH-1015 Lausanne, Switzerland
 - 22 INFN-Sezione di Lecce and Università Degli Studi di Lecce, I-73100 Lecce, Italy
 - 23 Institut de Physique Nucléaire de Lyon, IN2P3-CNRS, Université Claude Bernard, F-69622 Villeurbanne, France
 - 24 Centro de Investigaciones Energéticas, Medioambientales y Tecnológicas, CIEMAT, E-28040 Madrid, Spain^b
 - 25 INFN-Sezione di Milano, I-20133 Milan, Italy
 - 26 Institute of Theoretical and Experimental Physics, ITEP, Moscow, Russia
 - 27 INFN-Sezione di Napoli and University of Naples, I-80125 Naples, Italy
 - 28 Department of Natural Sciences, University of Cyprus, Nicosia, Cyprus
 - 29 University of Nijmegen and NIKHEF, NL-6525 ED Nijmegen, The Netherlands
 - 30 California Institute of Technology, Pasadena, CA 91125, USA
 - 31 INFN-Sezione di Perugia and Università Degli Studi di Perugia, I-06100 Perugia, Italy
 - 32 Carnegie Mellon University, Pittsburgh, PA 15213, USA
 - 33 Princeton University, Princeton, NJ 08544, USA
 - 34 INFN-Sezione di Roma and University of Rome, "La Sapienza", I-00185 Rome, Italy
 - 35 Nuclear Physics Institute, St. Petersburg, Russia
 - 36 University and INFN, Salerno, I-84100 Salerno, Italy
 - 37 University of California, San Diego, CA 92093, USA
 - 38 Dept. de Física de Partículas Elementales, Univ. de Santiago, E-15706 Santiago de Compostela, Spain
 - 39 Bulgarian Academy of Sciences, Central Lab. of Mechatronics and Instrumentation, BU-1113 Sofia, Bulgaria
 - 40 Center for High Energy Physics, Adv. Inst. of Sciences and Technology, 305-701 Taejeon, Republic of Korea
 - 41 University of Alabama, Tuscaloosa, AL 35486, USA
 - 42 Utrecht University and NIKHEF, NL-3584 CB Utrecht, The Netherlands
 - 43 Purdue University, West Lafayette, IN 47907, USA
 - 44 Paul Scherrer Institut, PSI, CH-5232 Villigen, Switzerland
 - 45 DESY-Institut für Hochenergiephysik, D-15738 Zeuthen, FRG
 - 46 Eidgenössische Technische Hochschule, ETH Zürich, CH-8093 Zürich, Switzerland
 - 47 University of Hamburg, D-22761 Hamburg, FRG
 - 48 National Central University, Chung-Li, Taiwan, China
 - 49 Department of Physics, National Tsing Hua University, Taiwan, China
- [§] Supported by the German Bundesministerium für Bildung, Wissenschaft, Forschung und Technologie
[‡] Supported by the Hungarian OTKA fund under contract numbers T019181, F023259 and T024011.
[¶] Also supported by the Hungarian OTKA fund under contract numbers T22238 and T026178.
^b Supported also by the Comisión Interministerial de Ciencia y Tecnología.
[#] Also supported by CONICET and Universidad Nacional de La Plata, CC 67, 1900 La Plata, Argentina.
[‡] Supported by Deutscher Akademischer Austauschdienst.
[◇] Also supported by Panjab University, Chandigarh-160014, India.
[△] Supported by the National Natural Science Foundation of China.

References

- [1] A. Zichichi *et al.*, Preprint INFN/AE-67/3; Lett. Nuovo Cimento **4** (1970) 1156; Nuovo Cimento **17 A** (1973) 383;
M. Perl *et al.*, Phys. Rev. Lett. **35** (1975) 1489.
- [2] See for example the review by A. Djouadi, J. Ng and T.G. Rizzo, SLAC-PUB-95-6772, in *Electroweak Symmetry Breaking and New Physics at the TeV Scale*, T. Barklow, S. Dawson, H.E. Habor and S. Siegrist, Singapore, World Scientific (1997).
- [3] L3 Collaboration, M. Acciarri *et al.*, Phys. Lett. **B 377** (1996) 304;
L3 Collaboration, M. Acciarri *et al.*, Phys. Lett. **B 412** (1997) 189.
- [4] ALEPH Collaboration, D. Buskulic *et al.*, Phys. Lett. **B 384** (1996) 439;
ALEPH Collaboration, R. Barate *et al.*, Phys. Lett. **B 405** (1997) 379;
DELPHI Collaboration, P. Abreu *et al.*, Phys. Lett. **B 396** (1997) 315;
DELPHI Collaboration, P. Abreu *et al.*, E. Phys. J. **C8** (1999) 41;
DELPHI Collaboration, P. Abreu *et al.*, Phys. Lett. **B444** (1998) 491;
OPAL Collaboration, G. Alexander *et al.*, Phys. Lett. **B 385** (1996) 433;
OPAL Collaboration, K. Ackerstaff *et al.*, Phys. Lett. **B 393** (1997) 217.
OPAL Collaboration, K. Ackerstaff *et al.*, Eur. Phys. J. **C 1** (1998) 45.
- [5] L3 Collaboration, B. Adeva *et al.*, Nucl. Instr. Meth. **A 289** (1990) 35;
M. Acciari *et al.*, Nucl. Instr. Meth. **A 351** (1994) 300;
M. Chemarin *et al.*, Nucl. Instr. Meth. **A 349** (1994) 345;
M. Adam *et al.*, Nucl. Instr. Meth. **A 383** (1996) 342;
G. Basti *et al.*, Nucl. Instr. Meth. **A 374** (1996) 293.
- [6] M. Gronau, C. Leung and J. Rosner, Phys. Rev. **D29** (1984) 2539.
- [7] S. Jadach and J. Kühn, Preprint MPI-PAE/PTh 64/86.
- [8] T. Sjöstrand, Comp. Phys. Comm. **82** (1994) 74.
- [9] S. Jadach, B.F.L.Ward and Z. Was, Comp. Phys. Comm. **79** (1994) 503.
- [10] M. Skrzypek *et al.*, Comp. Phys. Comm. **94** (1996) 216;
M. Skrzypek *et al.*, Phys. Lett. **B 372** (1996) 289.
- [11] R. Engel, Z. Phys. **C 66** (1993) 1657;
R. Engel and J. Ranft, Phys. Rev. **D 54** (1996) 4244.
- [12] F.A. Berends, P.H. Daverveldt and R. Kleiss, Nucl. Phys. **B 253** (1985) 421; Comp. Phys. Comm. **40** (1986) 271.
- [13] F.A. Berends, R. Kleiss and R. Pittau, Nucl. Phys. **B424** (1994) 308; Nucl. Phys. **B426** (1994) 344; Nucl. Phys. (Proc. Suppl.) **B37** (1994) 163; Phys. Lett. **B 335** (1994) 490;
R. Kleiss and R. Pittau, Comp. Phys. Comm. **83** (1994) 141.
- [14] The L3 detector simulation is based on GEANT Version 3.15. See R. Brun *et al.*, "GEANT 3", CERN DD/EE/84-1 (Revised), September 1987. The GHEISHA program (H. Fesefeldt, RWTH Aachen Report PITHA 85/02 (1985)) is used to simulate hadronic interactions.

- [15] V.F. Obraztsov, Nucl. Instr. Meth. **A 316** (1992) 388.
- [16] ALEPH Collaboration, D. Decamp *et al.*, Phys. Lett. **B 236** (1990) 511;
DELPHI Collaboration, P. Abreu *et al.*, Phys. Lett. **B 274** (1992) 230;
L3 Collaboration, B. Adeva *et al.*, Phys. Lett. **B 251** (1990) 321;
OPAL Collaboration, G. Alexander *et al.*, Z. Phys. **C 52** (1991) 200.
- [17] L3 Collaboration, M. Acciarri *et al.*, Eur. Phys. Journal **C 4**, (1998) 207.
- [18] L3 Collab., M. Acciarri *et al.*, CERN EP/99-024, to be published in Phys Lett **B**.

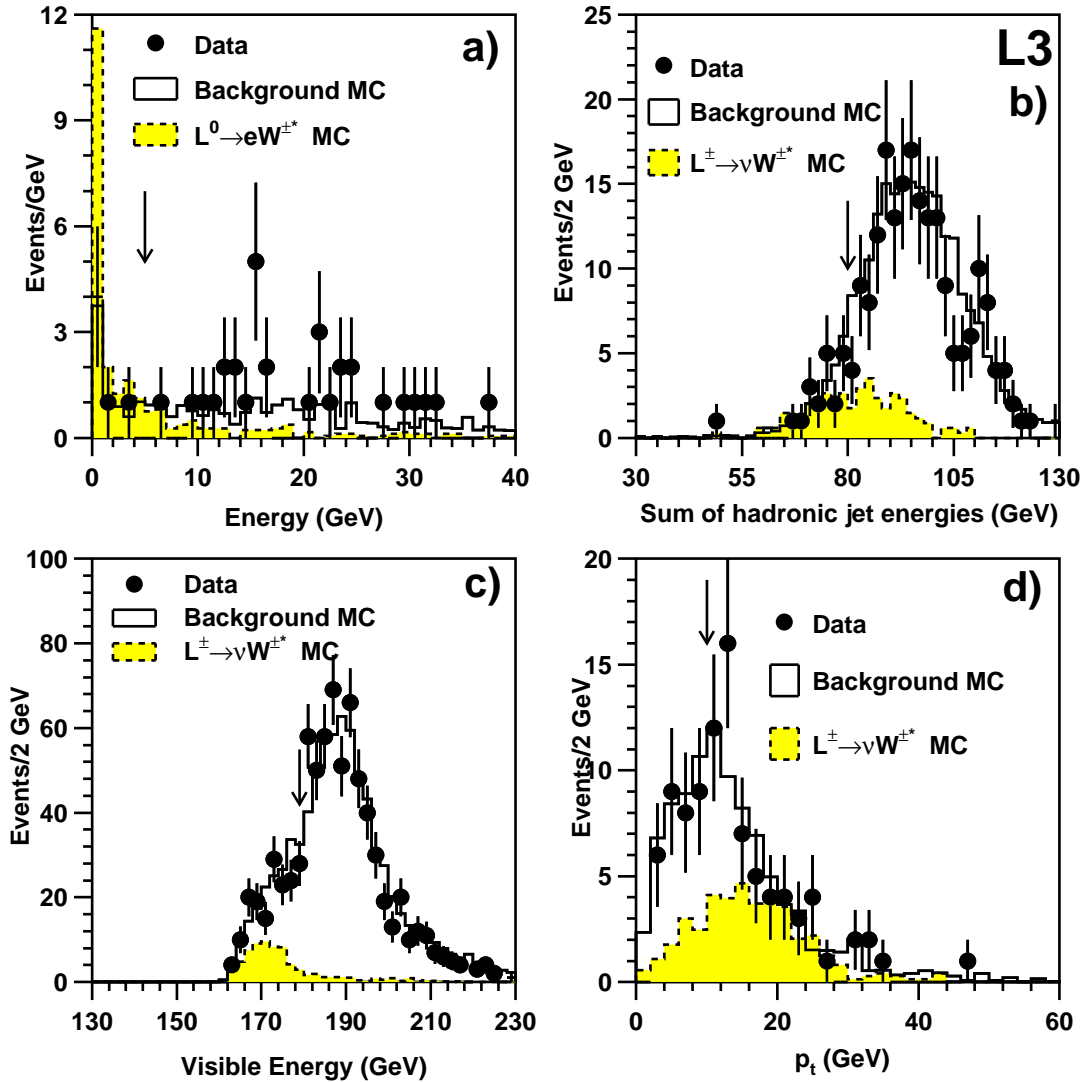


Figure 1: a) Energy in a 30° cone around the second most energetic electron candidate. b) The sum of the energies of the hadronic jets. c) Visible energy in the event. d) The distribution of the total transverse momentum, p_t . The dots are the data, the solid histogram is the background Monte-Carlo. The dashed line represents the simulated signal for $e^+e^- \rightarrow L\bar{L}$ from the TIPTOP Monte-Carlo. The normalization for the signal Monte-Carlo is scaled by a factor of 2 for better visibility. The arrows indicate the corresponding values of the applied cuts. In this case, all cuts on other quantities have been applied.

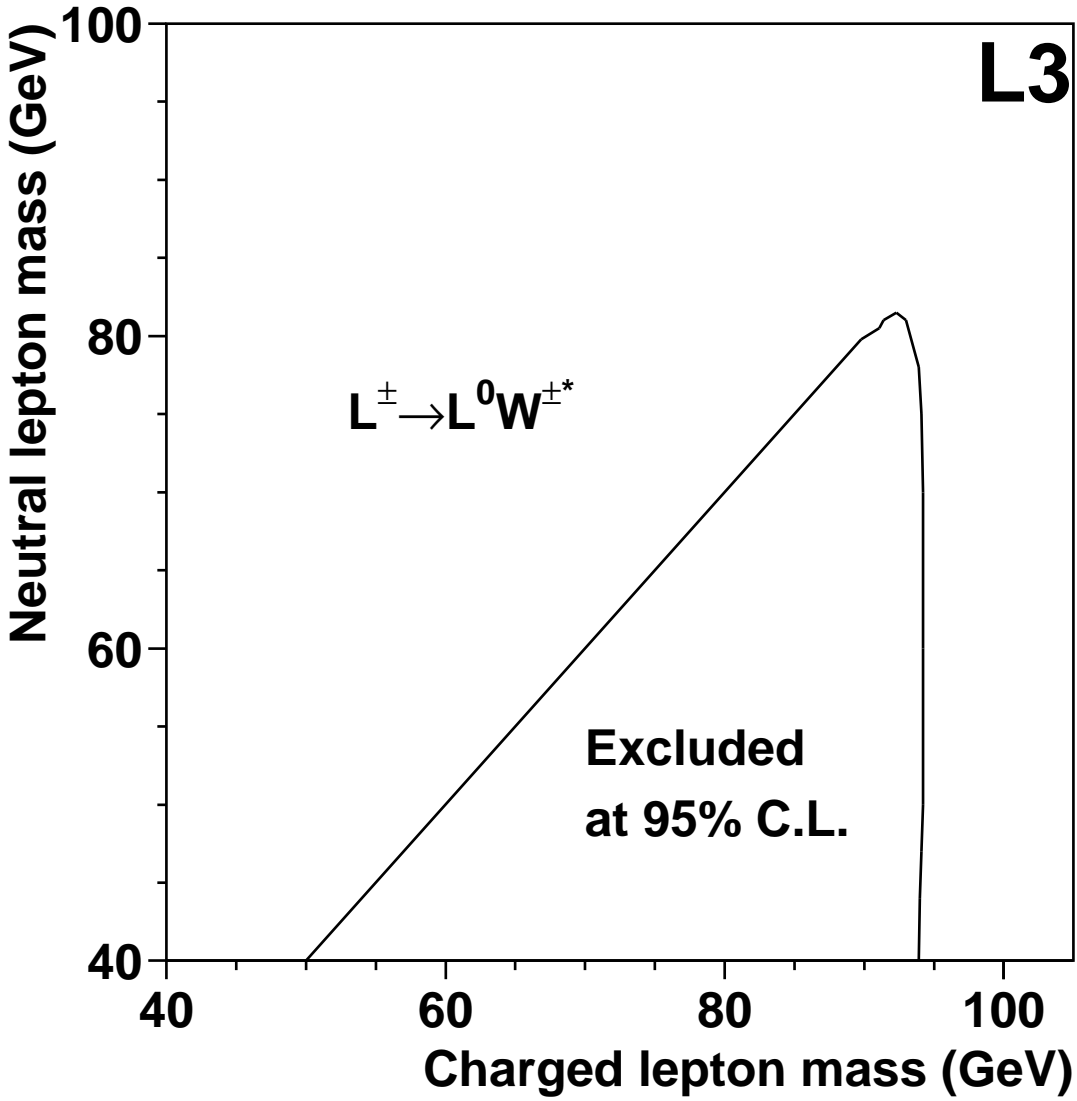


Figure 2: The 95% confidence level limit on the charged heavy lepton mass m_{L^\pm} and the associated neutral heavy lepton mass m_{L^0} assuming that the L^0 is stable.

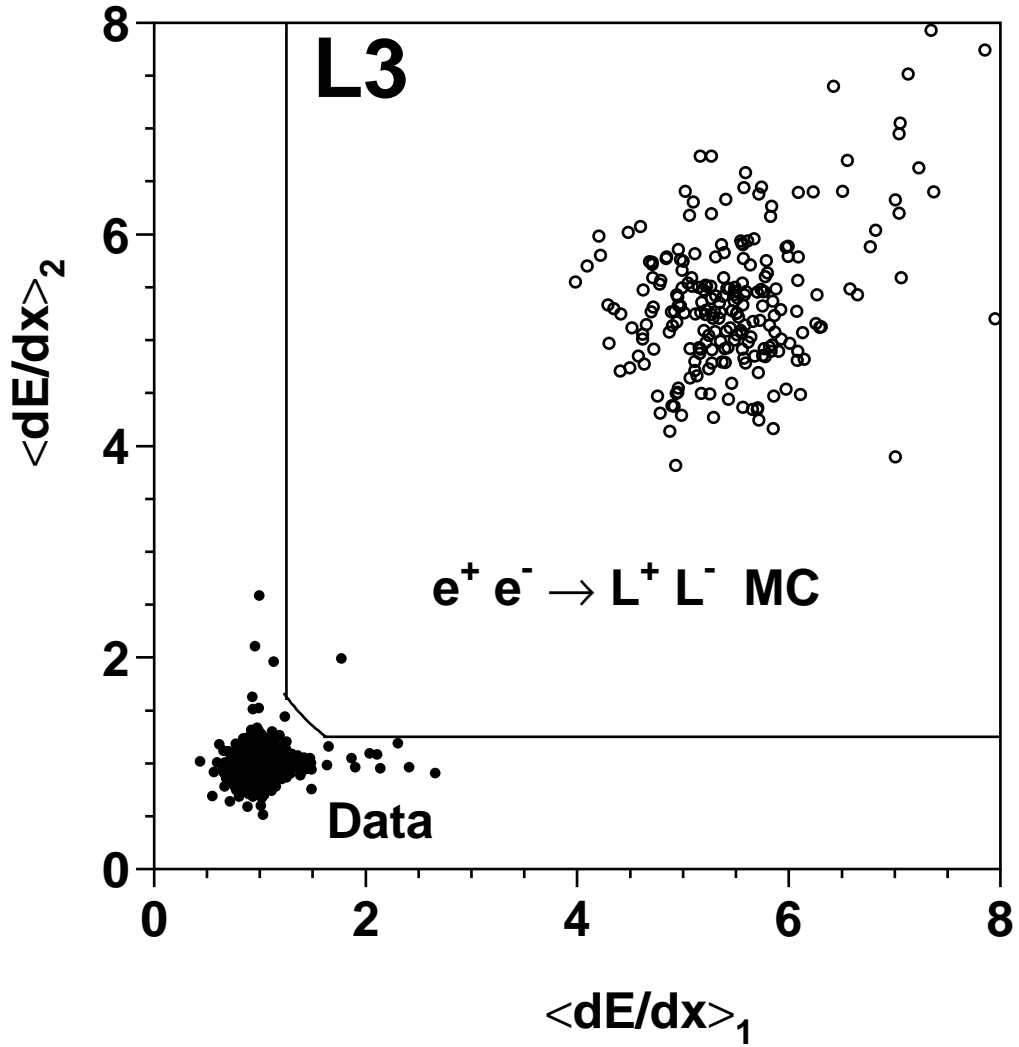


Figure 3: The normalized measured track energy loss of track 2 vs track 1 for the data (solid circles) taken at $\sqrt{s} = 189$ GeV and the simulated signal (arbitrary normalization) for a mass 93 GeV stable heavy lepton (open circles). The lines represent the applied cut.

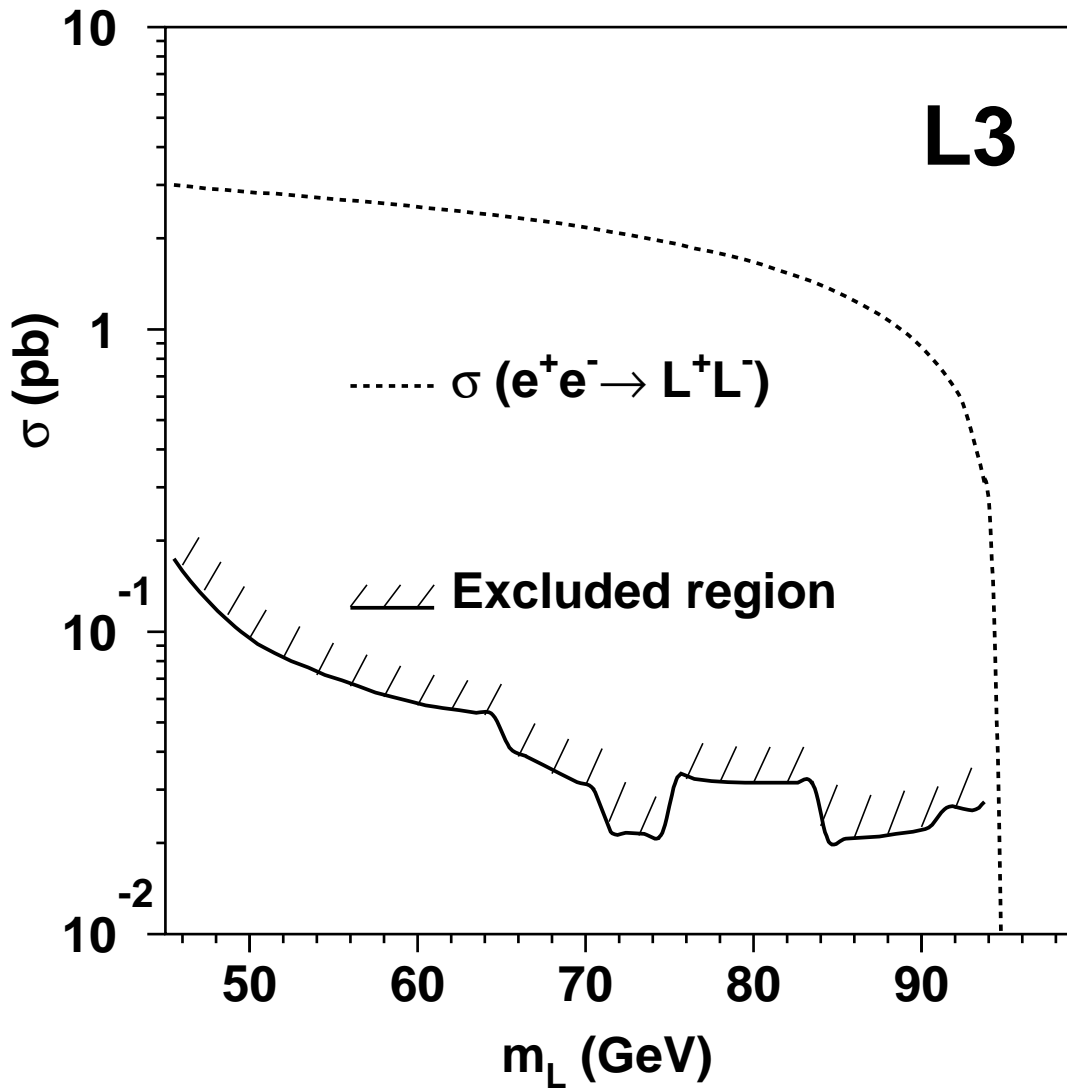


Figure 4: Upper limit of the production cross section for pair-production of stable charged heavy leptons in the L3 data at $\sqrt{s} = 133$ to 189 GeV as a function of mass. We do not determine the upper limit for masses greater than 93.5 GeV. The hatched area indicates the region excluded by our search. The dashed line represents the calculated pair-production cross section for heavy leptons at $\sqrt{s} = 189$ GeV from the TIPTOP Monte-Carlo.